Theory of polarization dependent intersubband transitions in *p*-type SiGe/Si self-assembled quantum dots

Yih-Yin Lin[a] and Jasprit Singh
Department of Electrical Engineering and Computer Science, University of Michigan, Ann Arbor, Michigan 48109-2122

(Received 3 October 2003; accepted 7 April 2004)

Electronic and optoelectronic properties of SiGe/Si self-assembled quantum dots are calculated by the eight-band **k·p** method with a revised set of parameters. The model confirms that the $Si_{1-x}Ge_x$ transforms to a type-II structure when x is greater than 0.25 and given accurate effective masses for Si and Ge. The polarization dependent absorption spectra show a behavior quite different from what is seen in conduction band intersubband transitions in self-assembled InGaAs/GaAs dots. In-plane or x-polarized absorption increases as germanium content is increased but z-polarized absorption is highest for low germanium content. It is also shown that the z-polarized absorption can be of the same magnitude as in the x-direction by adjusting the dot composition. We also clarify how the envelope functions and the Block parts of the electronic states contribute to the absorption spectra.
 [DOI: 10.1063/1.1755848]

I. INTRODUCTION

In recent years, self-assembled quantum dots based on the Stranski–Krastanov growth mode have been intensively studied due to their potential application in optical and electronic devices. Numerous studies on group III-V quantum dot systems such as InGaAs/GaAs,[1,2] InAs/InP,[3,4] and InAs/In(Ga,Al)As (Ref. 5) have been reported both experimentally and theoretically for a wide range of dot sizes and shapes. Group IV quantum structures such as SiGe/Si and SiGeC/Si are of particular interest since the possibility of various device applications and the compatibility with the silicon-based technology. Unlike group III-V materials, a main feature that characterizes this system is the indirect energy band gap in both Si and Ge. Moreover, the energy band-gap difference in the $Si_{1-x}Ge_x/Si$ appears mostly in the valence band since the conduction band offset is reduced by the strain in SiGe heterostructure.[6] Photoluminescence (PL) studies of the as-grown SiGe dots show that the band alignment is that of a type-II structure, where the conduction band is higher in the dots than in the Si matrix, for high germanium content. This property prohibits quantum confinement of both electrons and holes, thus limiting possible electronic applications such as single-electron transistors and quantum computers.[7] It has been shown that the band alignment transforms to type-I for lower Ge content in the $Si_{1-x}Ge_x/Si$ quantum well structure. The cross-over composition has been repeated as 0.25 by Ref. 8 and 0.16 by Ref. 9. Post-growth thermal processes like annealing have been used to reach a proper germanium composition and obtain the type-I structure by silicon interdiffusion.[10]

In addition to the band alignment issue, the indirect band-gap nature of a SiGe/Si quantum structure also limits its optical application due to subdued band-to-band transition since direct radiative recombination of photoexcited carriers is prohibited. The photoluminescence (PL) emission of the SiGe quantum structure is therefore relatively weak and long-lived. Therefore, it is the optical transitions of holes between valence subbands that draws the most attention in published works. In this study, we will present a calculation of the energy-band structure and valence band intersubband optical transitions of a strained indirect gap SiGe/Si QD system. Theoretically, the tight-binding methods combined with empirical pseudopotential models,[11] and the **k·p** theory[12,13] have been used to perform the calculation of bulk semiconductors. In this calculation, we will use the **k·p** method with the deformation potential theory to include the strain effects in the quantum dot structure. The **k·p** approach for a full band structure in bulk indirect gap materials has been approximated by a linear-muffin-tin method,[14] a five-level model,[15] or sp^3s^*‘‘d’’ method,[16] each containing a 14×14, 16×16, or 20×20 Hamiltonian, respectively. The advantage of the full **k·p** method is to obtain a precise band structure all over the Brillouin zone and is applicable to both direct and indirect gap semiconductors. However in this study, we are only concerned about the carrier properties near the direct gap hence an extensive Hamiltonian is not crucial in the calculation.

So far the calculation of a quantum confined SiGe/Si heterostructure is performed based on a three-level **k·p** description or a six-band method including spin to solve the valence band structure.[17,18] Dekel *et al.*[19] reported an eight-band **k·p** approach for the Ge/Si quantum dot system and revealed detailed profiles of the heavy holes, light holes, and split-off bands, but the approach lacked an accurate description of the conduction band. Here we use an eight-band Hamiltonian with modified Luttinger-like parameters following Ref. 20 as to take into account the influence of remote bands. In this article, we will report theoretically calculated energy band levels in a SiGe/Si quantum dot and then discuss the intersubband transitions. In particular, we will cal-

[a]Electronic mail: ylin@engin.umich.edu

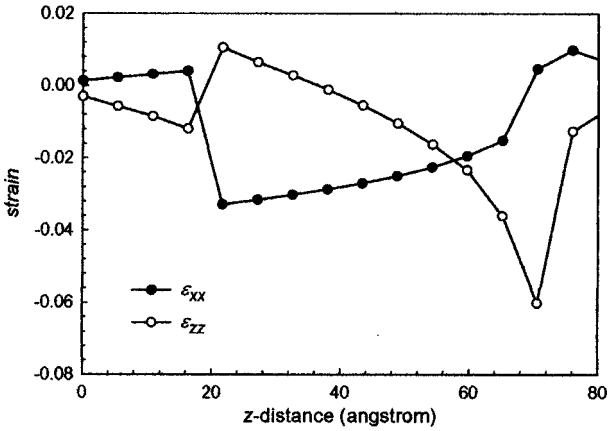

FIG. 1. Strain profiles of a Ge/Si quantum dot obtained by VFF model. The dot dimension is 59.74 Å in height and the base-to-height ratio of 2.

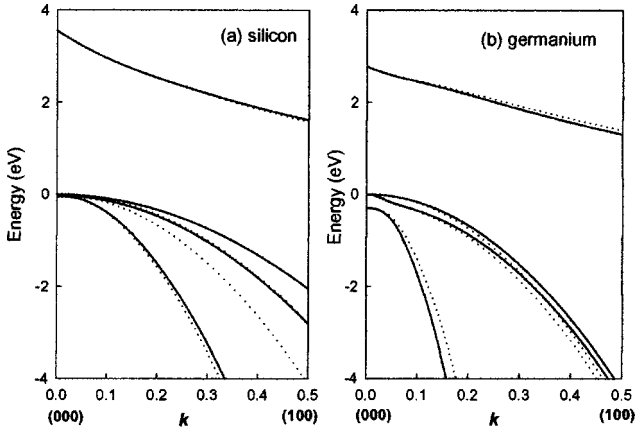

FIG. 2. Schematic band structures of (a) Si and (b) Ge simulated by eight-band **k·p**. Solid lines show the results using the values in this simulation and dotted lines are obtained by using the P-B Luttinger parameters.

culate polarization dependence of valence band intersubband transitions.

II. THEORY AND RESULTS

The model we use for the shape of the dot is a square-based pyramidal shaped $Si_{1-x}Ge_x$ dot grown on the unstrained (100) silicon substrate. It is experimentally reported that SiGe/Si quantum dots grown by molecular beam epitaxy have a range of sizes.[21,22] The range appears to depend upon growth techniques and growth conditions. It is possible that surface preparation also influences dot sizes. It is found that the square-based pyramids have a base-to-height ratio roughly of 4-5:1.[21,22] In our calculation, the dot structure we examine is pyramidal with a height of 58.4 Å and a base width of 237.9 Å. The dot is chosen to have height-to-width ratio that is consistent with experimental observation. As noted above, experimental reported dots vary in sizes so our results should be viewed as providing a general guidance. The actual values of transition energies and the oscillation strength will vary if the dot size were altered. In the simulation we assume that the Ge composition x is uniform in the dot and the dot is embedded in pure silicon.

Built-in strain is a key factor in determination of the band structure in self-assembled structures. In this article, we determine the strain profile by the valence force field (VFF) method, which involves a minimal energy configuration of the atomic structure. It has been argued that the VFF method is not appropriate for small dots with a base length less than 10 nm (Refs. 23 and 24) while the Stillinger–Weber potential model is recommended for such small structures. However it has been shown that both models are in good agreement for the strain calculation in the covered/capped structure.[25] Parameters in the Keating potentials of Si and Ge used in the VFF method are cited from Refs. 26 and 27. The tolerance for the convergence criterion of minimization iteration is set to be 10^{-8} eV per atom. The strain profiles at the dot center is shown in Fig. 1.

The $8\times8\,\Gamma_6\Gamma_7\Gamma_8$ effective Hamiltonian has been applied to direct band-gap semiconductors and is shown to accurately predict both bulk and quantum dot energy spectrum.[24] As is well known, the band gaps of silicon and germanium occur at X and L points, respectively. We need to go beyond the Γ point and use Luttinger-like parameters considering the influence of remote bands. We obtain the Luttinger-like parameters via a second-order perturbation theory after Ref. 20, and the values are listed in Table I. The widely used Luttinger parameters introduced by Pidgeon and Brown[28] (here we refer to as P-B Luttinger parameters) are also given in the table for comparison. The calculated valence band profiles of bulk Si and Ge by our modified Luttinger-like parameters and by the P-B Luttinger parameters are shown in Fig. 2. The modified parameters yield a better fit to the effective masses at the Γ point.

The strain Hamiltonian needs to take into account the deformation potentials which cause hydrostatic shift (a_c or a_v) and the splitting (b) at the minimum Δ point. It is then necessary to include Ξ_u besides Ξ_d at the Γ-point under [001]-direction biaxial stress. A list of all the parameters used in the calculation is given in Table II. The overall Hamiltonian is solved by an implicitly restarted Arnoldi/Lanczos method (ARPACK program), an eigenvalue solver developed by Rice University.

TABLE I. Numerical values of Luttinger-like parameters used in the simulation (in superscripts a) and the Luttinger parameters in Kane's paper (Ref. 29) defined by Pidgeon and Brown (Ref. 28) (in superscripts b), and the effective masses obtained by both methods.

	γ_1	γ_2	γ_3	$m_{e,l}$	$m_{e,t}$	m_{hh}	m_{lh}	m_{so}
Silicon[a]	4.144	0.432	1.362	1.019	0.169	0.408	0.169	0.254
Silicon[b]	4.285	0.339	1.446	1.019	0.170	0.373	0.161	0.339
Germanium[a]	15.97	5.761	5.382	···	···	0.286	0.047	0.056
Germanium[b]	13.38	4.240	5.690	···	···	0.253	0.055	0.073

TABLE II. Constants used in the band-structure simulations. E_p is the optical transition matrix element. m_e is the bulk electron mass given as a fraction of the free-electron mass m_0. $E_{g,\mathrm{ind}}$ is the indirect gap energy. a_v, a_{ind}, and a_{dir} are the hydrostatic strain potentials for the valence band, the indirect gap, and the direct gap in the conduction band. b_v is the valence band shear deformation potential.

	E_p (eV)	m_e (m_0)	$E_{g,\mathrm{ind}}$ (eV)	a_v (eV)	a_{ind} (eV)	a_{dir} (eV)	b_v (eV)
Silicon	21.6	0.528	1.17	2.46	1.72	−0.48	−2.1
Germanium	26.3	0.038	0.744	1.24	−2.78	−9.48	−2.9

The energy band gap in the SiGe quantum dots as a function of the germanium content x is shown in Fig. 3. As mentioned earlier, the kind of band alignment will convert from type-I to type-II at a certain composition. We have found confined states in the conduction band when x is up to 0.25 with an effective band gap of 1.085 eV. This x value is consistent with what has been found in SiGe/Si quantum wells.[8] Above $x=0.25$, the band alignment of SiGe becomes a type-II and the band gap is estimated from the conduction band edge in Si substrate to the first excited hole state in SiGe. Here the band edge is taken from the substrate instead of from the capping layer to eliminate the strain effects on Si at the interface. The range of band-gap values is close to what is found from literature, but as mentioned earlier, the PL spectrum is very weak due to prohibited direct radiation and the severe Si interdiffusion affects the PL result. The calculated energy changes due to intersubband transitions between the jth-excited and the ground hole states are given in Table III as a function of germanium content in the dot.

The absorption coefficient profiles due to intersubband hole transitions under vertical incidence and lateral incidence are shown in Figs. 4(a) and 4(b). The intersubband absorption coefficient α of a photon with energy $\hbar w$ in a quantum dot layer is

$$\alpha(\hbar w)=\frac{\pi e^2\hbar}{\epsilon_0 n_0 c m_0^2 V_{\mathrm{av}}}\frac{1}{\hbar w}\sum_{fi}|\mathbf{a}\cdot\mathbf{P}_{fi}|N(\hbar w), \tag{1}$$

where c is the speed of light, ϵ_0 is the dielectric constant of vacuum, n_0 is the refractive index, and V_{av} is the average dot volume. $\mathbf{a}$ is the polarization of the light, and $N(\hbar w)$ is the electron joint density of states for the initial and final states.

$$N(\hbar w)=\frac{1}{\sqrt{2\pi}\sigma}\exp\left[\frac{(E_{fi}-\hbar w)^2}{(2\sigma)^2}\right], \tag{2}$$

where E_{fi} is the energy separation between states f and i, and σ is the linewidth of the transition, which is taken as 20 meV in the simulation. The momentum matrix element $\mathbf{P}_{fi}$ between the initial and final states

$$|\mathbf{a}\cdot\mathbf{P}_{fi}|=\frac{|\langle u_c|p_x|ux\rangle|^2}{6}|\mathbf{a}\cdot\mathbf{P}_{fi}|^2_{\mathrm{env}}, \tag{3}$$

where the first part is due to the band-edge Block parts and the second part is due to the envelope wave function overlap.

The absorption coefficient (α) is calculated with a linewidth (σ) of 20 meV and the dot density is chosen to be $10^{-10}\,\mathrm{cm}^{-2}$. The optical absorption scales inversely with the linewidth. Comparing the position of the peak values in Fig. 4(a) with Table III results, it is found that the x-polarized absorption is due to the transition between E_{V1} and E_{V4} or E_{V3}. Likewise the z-polarized absorption results from the $E_{V5}\rightarrow E_{V1}$ transition. Figure 4(a) also shows a significant transition from E_{V6} to E_{V1} in high germanium content dots, caused by the strong matrix element between these two states.

We examine how much contribution to the absorption strength comes from the Bloch part of the electronic state and how much comes from the envelope part. We find that for the x-polarized absorption, in quantum dots is dominated by the band-edge Block parts in the momentum matrix while the envelope function overlap is comparable to the Block parts for the z-polarized absorption. For low Ge content, the Bloch part is relatively small under vertical incidence but the envelope part is fairly large under lateral illumination. Therefore Figs. 4(a) and 4(b) exhibit different tendencies with germanium composition in the dot. It should also be noticed that

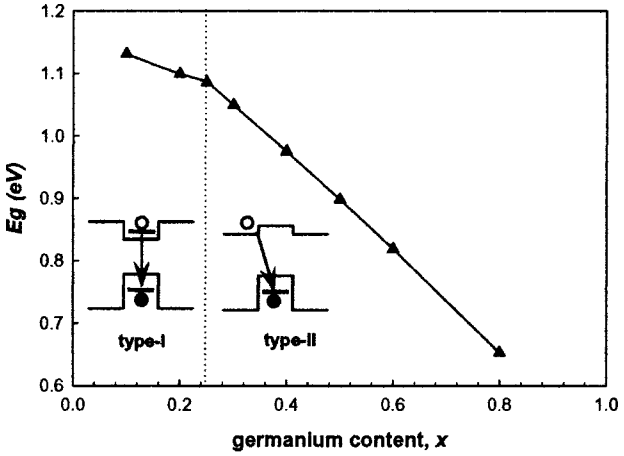

FIG. 3. Calculated energy band-gap values as a function of germanium content in the dot. The solid line indicates the transition of band-gap alignment.

TABLE III. Calculated hole subband energy differences of SiGe/Si quantum dots.

Ge content	20%	40%	50%	60%	80%	100%
$E_{V2}-E_{V1}$, meV	12.32	20.84	23.89	26.48	30.59	32.96
$E_{V3}-E_{V1}$, meV	25.06	38.52	43.21	47.00	53.19	58.35
$E_{V4}-E_{V1}$, meV	28.34	39.68	44.02	48.03	54.70	59.43
$E_{V5}-E_{V1}$, meV	37.03	58.61	65.94	71.73	80.29	84.95
$E_{V6}-E_{V1}$, meV	40.36	62.34	71.27	78.83	90.25	98.20
$E_{V7}-E_{V1}$, meV	46.20	66.08	74.24	81.77	94.27	101.92
$E_{V8}-E_{V1}$, meV	53.22	80.48	89.67	96.52	106.77	113.59

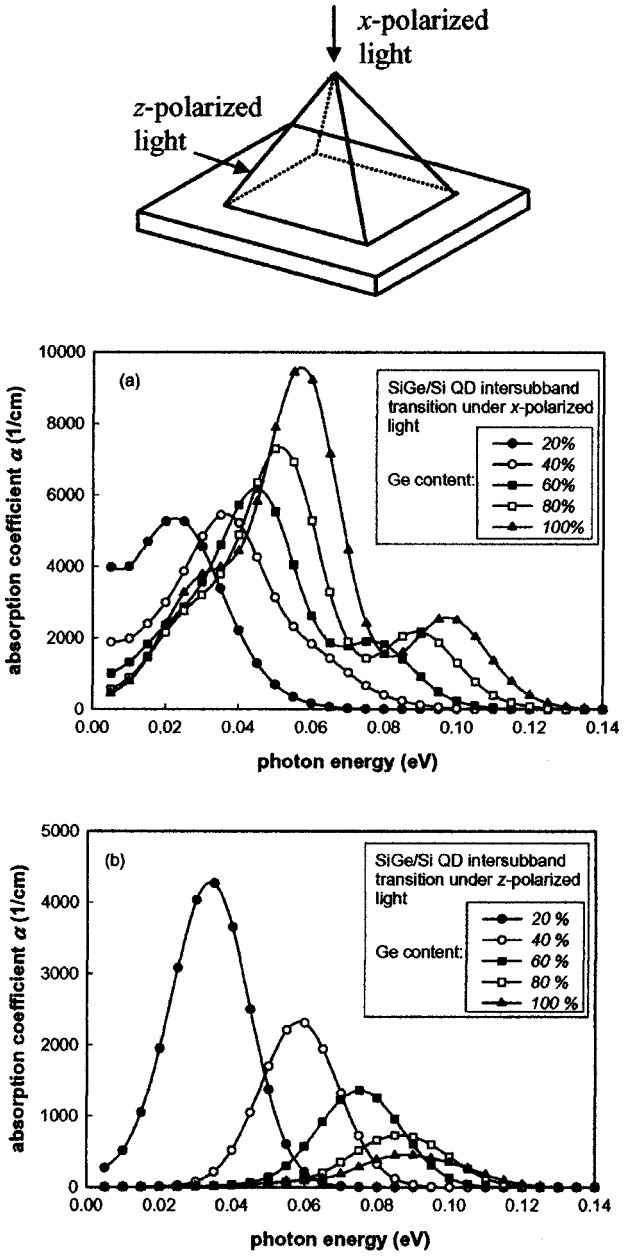

FIG. 4. Intersubband absorption spectra for SiGe/Si dots with various Ge composition. (The linewidth is taken to be 20 meV.) (a) *x*-polarized absorption. (b) *z*-polarized absorption.

for low germanium content, the *z*-polarized absorption can be of the same magnitude as the *x*-polarized absorption, which is not usually observed in the *n*-type quantum dot structure. Thus a quantum dot device which can detect polarized lights in both directions can be built if the $Si_{1-x}Ge_x$/Si dots with a composition distribution can be assembled. Note that these selection rules are quite different from what is observed in the conduction band of InGaAs/GaAs self-assembled dots. For the InGaAs/GaAs dots the *z*-polarization absorption dominates.

III. CONCLUSION

In conclusion, we have theoretically investigated the band structure and valence band intersubband transitions of SiGe/Si QDs. We have developed an eight-band **k·p** model for calculation of the band gap and the intersubband hole transitions. There is no confined conduction band state as the Ge content increases above 25% and band alignment changes from type-I to type-II. In-plane *x*-polarized intersubband absorption increases with Ge content. The magnitude of the *z*-polarized absorption is strong and the largest (at the lowest Ge content) is almost half of the *x*-polarized absorption. Our study shows that SiGe/Ge dots can be used for both in-plane and vertical incident long wavelength detectors.

Our study provides an insightful view to the electronic structure of a SiGe/Si quantum dot. Due to the lack of theoretical and experimental references, we have made several approximation for 8×8 **k·p** simulation. We expect that experimentalists will measure polarization dependence of intersubband absorption as a function of Ge content so that some of the interesting and potentially useful predictions of this article can be verified.

ACKNOWLEDGMENTS

This work was supported by a U.S. Army MURI program (the CENTROID program). Discussion with Professor K. L. Wang and his group at the University of California, Los Angeles has been extremely helpful.

[1] P. M. Petroff and G. Medeiros-Ribeiro, MRS Bull. **1996**, 50.
[2] R. P. Mirin, J. P. Ibbetson, K. Nishi, A. C. Gossard, and J. E. Bowers, Appl. Phys. Lett. **67**, 3795 (1995).
[3] V. M. Ustinov, E. R. Weber, S. Ruvimov, Z. Liliental-Weber, A. E. Zhukov, A. Yu. Egorov, A. R. Kovsh, A. F. Tsatsulnikov, and P. S. Kopev, Appl. Phys. Lett. **72**, 362 (1998).
[4] H. Pettersson, R. J. Warburton, J. P. Kotthaus, N. Carlsson, W. Seifcrt, M.-E. Pistol, and L. Samuelson, Phys. Rev. B **60**, 11 289 (1999).
[5] M. Grundmann, N. N. Ledentsov, R. Heitz, L. Eckey, J. Christen, J. Böhrer, D. Bimberg, S. S. Ruvimov, P. Werner, U. Richter, J. Heydenreich, V. M. Ustinov, A. Yu. Egorov, A. E. Zhukov, Kopev, and Zh. I. Alferov, Phys. Status Solidi A **188**, 249 (1995); M. Grundmann, Adv. Solid State Phys. (Festkoerperprobleme) **35**, 123 (1996).
[6] C. G. Van de Walle, Phys. Rev. B **39**, 1871 (1989).
[7] K. L. Wang, J. L. Liu, and G. Jin, First International Workshop on New Group IV Semiconductors (Japan, 2001), p. 103.
[8] G. A. Northrop, J. F. Morar, D. J. Wolford, and J. A. Bradley, J. Vac. Sci. Technol. B **10**, 2018 (1992).
[9] S. Fukatsu and Y. Shiraki, Appl. Phys. Lett. **63**, 2378 (1993).
[10] J. Wan, Y. H. Luo, Z. M. Jiang, G. Jin, J. L. Liu, K. L. Wang, X. Z. Liao, and J. Zou, Appl. Phys. Lett. **79**, 1980 (2001).
[11] A. Zunger and M. L. Cohen, Phys. Rev. B **20**, 4082 (1979).
[12] D. Gershoni, C. H. Henry, and G. A. Baraff, IEEE J. Quantum Electron. **29**, 2433 (1993).
[13] T. B. Bahder, Phys. Rev. B **45**, 1629 (1992).
[14] M. Cardona, N. E. Christensen, and G. Fasol, Phys. Rev. B **38**, 1806 (1988).
[15] P. Pfeffer and W. Zawadzki, Phys. Rev. B **53**, 12 813 (1996).
[16] N. Cavassilas, F. Aniel, K. Boujdaria, and G. Fishman, Phys. Rev. B **64**, 115 207 (2001).
[17] J. M. Hinckley and J. Singh, Phys. Rev. B **41**, 2912 (1990).
[18] K. Yeom, J. M. Hinckley, and J. Singh, J. Appl. Phys. **80**, 6773 (1996).
[19] E. Dekel, E. Ehrenfreund, D. Gershoni, P. Boucaud, I. Sagnes, and Y. Campidelli, Phys. Rev. B **56**, 15 734 (1997).
[20] K. Boujdaria, S. Ridene, and G. Fishman, Phys. Rev. B **63**, 235 302 (2001).
[21] Y. Zhang, M. Floyd, J. Drucker, and G. L. Kellogg, J. Appl. Phys. **90**, 4748 (2001).
[22] X. Z. Liao, J. Zou, D. J. H. Codkayne, Z. M. Jiang, X. Wang, and R. Leon, Appl. Phys. Lett. **77**, 1304 (2000).
[23] M. A. Cusack, P. R. Briddon, and J. Jaros, Phys. Rev. B **54**, R2300 (1996).
[24] H. Jiang and J. Singh, Physica E (Amsterdam) **2**, 614 (1998).

[25] Y. Kikuchi, H. Sugii, and K. Shintani, J. Appl. Phys. **89**, 1191 (2001).
[26] M. Schulz and R. Blachnik, in *LANDOLT-BÖRNSTEIN Numerical Data and Functional Relationships in Science and Technology*, New Series, edited by O. Madelung (Springer, New York, 1982), III, Vol. 17a, p. 61.
[27] M. S. Skolnick and R. Blachnik, in *LANDOLT-BÖRNSTEIN Numerical Data and Functional Relationships in Science and Technology*, New Series, edited by O. Madelung (Springer, New York, 1982), III, Vol. 17a, p. 103.
[28] C. R. Pidgeon and R. N. Brown, Phys. Rev. B **146**, 575 (1966).
[29] E. O. Kane, J. Phys. Chem. Solids **1**, 249 (1957).